

UCSF

UC San Francisco Previously Published Works

Title

970: DISCRETE FIBROBLAST SUBSETS NURTURE GASTRIC CARCINOGENESIS

Permalink

<https://escholarship.org/uc/item/6qb2c76m>

Journal

Gastroenterology, 162(7)

ISSN

0016-5085

Authors

Lee, Su-Hyung
Panta, Ela W Contreras
Gibbs, David L
[et al.](#)

Publication Date

2022-05-01

DOI

10.1016/s0016-5085(22)60549-3

Peer reviewed

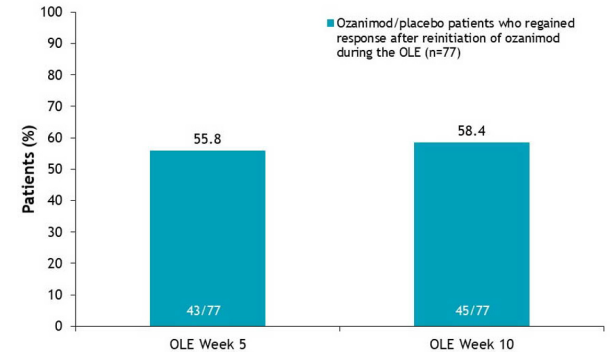
Table 1. Baseline demographics and disease characteristics in the tofacitinib UC clinical program, by cohort

	Maintenance Cohort (52 weeks)			Overall-P3b4 Cohort (52.8 years)		
	Placebo (N=198; 100.4 PY)	Tofacitinib 5 mg BID (N=198; 146.2 PY)	Tofacitinib 10 mg BID (N=196; 154.3 PY)	PD Tofacitinib 5 mg BID (N=202; 783.1 PY)	PD Tofacitinib 10 mg BID (N=955; 2,216.6 PY)	Tofacitinib All (N=1,157; 2,999.7 PY)
Baseline demographics and clinical characteristics						
Age (years), mean (SD) ^a	43.4 (14.0)	41.9 (13.7)	43.0 (14.4)	44.5 (14.5)	46.6 (13.7)	41.3 (13.9)
Total Mayo score, mean (SD) ^b	3.3 (3.8)	3.1 (4.3)	3.4 (4.3)	7.8 (2.5)	8.3 (3.8)	8.8 (2.0)
Disease duration (years), mean (SD) ^b	8.8 (7.5)	8.3 (7.2)	8.7 (7.0)	8.3 (6.5)	8.2 (7.1)	8.2 (7.0)
Prior TNF inhibitor use, n (%) ^c	89 (44.9)	83 (41.9)	92 (46.9)	84 (41.6)	499 (54.1)	583 (51.3)
Corticosteroid use at baseline, n (%) ^c	109 (55.0)	101 (51.0)	86 (43.9)	82 (40.6)	441 (46.2)	523 (45.2)

Table 2. IRs (unique pts with events/100 PY of exposure) for AEs, deaths, and AEs of special interest in the tofacitinib UC clinical program, by cohort

	Maintenance Cohort (52 weeks)			Overall-P3b4 Cohort (52.8 years)		
	Placebo (N=198; 100.4 PY)	Tofacitinib 5 mg BID (N=198; 146.2 PY)	Tofacitinib 10 mg BID (N=196; 154.3 PY)	PD Tofacitinib 5 mg BID (N=202; 783.1 PY)	PD Tofacitinib 10 mg BID (N=955; 2,216.6 PY)	Tofacitinib All (N=1,157; 2,999.7 PY)
AEs						
Pts with AEs, n (%)	149 (75.3)	141 (72.2)	156 (79.6)	189 (93.8)	808 (84.1)	992 (85.7)
Pts with serious AEs, n (%)	13 (6.6)	10 (5.1)	11 (5.6)	44 (21.8)	200 (20.9)	244 (21.1)
Deaths, n (%) IR [95% CI] ^d	0 (0.0)	0 (0.0)	0 (0.0)	0 (0.0)	7 (0.7)	7 (0.6)
Infections, n (%) IR [95% CI]^e						
Upper respiratory tract infections	21 (10.6)	2 (1.0)	1 (0.5)	10 (5.0)	42 (4.4)	52 (4.5)
All herpes (non-oncogenic and serious)	1.94 (0.23, 2.00)	1.35 (0.16, 4.87)	0.64 (0.02, 3.54)	1.23 (0.02, 2.29)	1.84 (3.33, 2.49)	1.60 (1.26, 2.31)
Herpes zoster	0.97 (0.02, 5.42)	2.05 (0.42, 6.00)	6.64 (1.19, 12.22)	3.00 (1.38, 4.54)	3.41 (2.67, 4.29)	3.30 (2.67, 4.04)
Herpes zoster OIs	0.97 (0.02, 5.42)	1.36 (0.16, 4.92)	2.60 (0.71, 6.65)	1.03 (0.45, 2.04)	1.02 (0.65, 1.53)	1.03 (0.70, 1.46)
Malignancies, n (%) IR [95% CI]^f						
Malignancies (excluding NSMC)	1 (0.5)	0 (0.0)	0 (0.0)	5 (2.5)	21 (2.3)	26 (2.3)
NSMC	0.97 (0.02, 5.39)	0.00 (0.00, 2.48)	0.00 (0.00, 2.35)	0.62 (0.20, 1.45)	0.92 (0.57, 1.41)	0.84 (0.55, 1.24)
MACI, n (%) IR [95% CI]^g						
MACI	0 (0.0)	1 (0.5)	1 (0.5)	4 (2.0)	5 (0.5)	9 (0.8)
VTE, n (%) IR [95% CI]^h						
VTE	1 (0.5)	0 (0.0)	0 (0.0)	0 (0.0)	1 (0.1)	1 (0.1)
DVT	0.97 (0.02, 5.39)	0.00 (0.00, 2.48)	0.00 (0.00, 2.35)	0.00 (0.00, 0.46)	0.04 (0.00, 0.24)	0.03 (0.00, 0.18)
PE	1 (0.5)	0 (0.0)	0 (0.0)	0 (0.0)	6 (0.6)	6 (0.5)
 gastrointestinal perforations, n (%) IR [95% CI]ⁱ						
GI perforations	0.97 (0.02, 5.39)	0.00 (0.00, 2.48)	0.00 (0.00, 2.35)	0.00 (0.00, 0.46)	0.20 (0.01, 0.57)	0.07 (0.01, 0.28)

Figure. Symptomatic clinical response^a at OLE weeks 5 and 10



^aA reduction from baseline in the partial Mayo Score of ≥1 point and ≥30%, and ≥1 point decrease in RBS or absolute RBS ≤1. OLE, open-label extension; RBS, rectal bleeding score.

969

RECAPTURE OF RESPONSE WITH OZANIMOD IN PATIENTS WITH MODERATELY TO SEVERELY ACTIVE ULCERATIVE COLITIS WHO WITHDREW THERAPY: DATA FROM THE TRUE NORTH OPEN-LABEL EXTENSION STUDY
 Anita Afzali, Michael V. Chiorean, Garrett Lawlor, Mark T. Osterman, Devrim Eren, Arteid Memaj, Remo Panaccione, Subrata Ghosh

Introduction: True North (NCT02435992) was a 52-week, phase 3, randomized, double-blind, placebo-controlled trial of ozanimod, a sphingosine 1-phosphate receptor modulator, in adults with moderately to severely active UC. The aim of this post-hoc analysis was to assess the response recapture rate upon reinitiation of ozanimod in the True North open-label extension (OLE) in patients who initially had clinical response to ozanimod at week 10 but subsequently had disease relapse during maintenance following ozanimod withdrawal.

Methods: In True North, patients were randomized 2:1 to receive double-blind ozanimod 0.92 mg (equivalent to ozanimod HCl 1 mg) or placebo (Cohort 1) or open-label ozanimod 0.92 mg (Cohort 2). Those who had clinical response to ozanimod at Week 10 were re-randomized 1:1 to receive ozanimod or placebo in a maintenance period. Patients in the maintenance period could enter the open-label extension (OLE) at Week 52 or after disease relapse. This analysis examined patients who achieved clinical response with ozanimod at week 10 and who received open-label reinduction with ozanimod after relapsing on placebo during the maintenance period. Disease relapse was defined as having a partial Mayo score ≥4 points and an increase of ≥2 points from week 10 with an endoscopic score of ≥2 points and exclusion of other causes of an increase in disease activity. The final decision to discontinue the patient early for entry into the OLE was based on investigator discretion. Symptomatic clinical response, defined as a reduction from baseline in the partial Mayo Score of ≥1 point and ≥30% with at least 1 point decrease in rectal bleeding score (RBS) or absolute RBS ≤1, was assessed at weeks 5 and 10 post-reinduction of ozanimod in the OLE (which included a 1-week dose escalation period). **Results:** A total of 77 patients reinitiated ozanimod treatment in the OLE after experiencing disease relapse following ozanimod withdrawal. These patients had a mean age of 40.2 years, 88.3% had prior corticosteroid use and 46.8% had prior TNF inhibitor use at induction baseline. Of these patients, 56% (43/77) achieved symptomatic clinical response at OLE week 5, and this rate was maintained at OLE week 10 (58%, 45/77; **Figure**). **Conclusion:** Almost 60% of patients who relapsed after ozanimod withdrawal during the randomized maintenance period of True North recaptured symptomatic clinical response by OLE week 10. Most patients recaptured response as early as 5 weeks of re-initiation of ozanimod during the OLE.

970

DISCRETE FIBROBLAST SUBSETS NURTURE GASTRIC CARCINOGENESIS
 Su-Hyung Lee, Ela W. Contreras Panta, David L. Gibbs, Yoonyoung Won, Jimin Min, Changting Zhang, Lorenzo E. Ferri, Veena Sangwan, Ioannis Ragoussis, Sophie Camilleri-Broet, Joseph Caruso, Michael Strasser, Philippe D. Gascard, Sui Huang, Thea D. Tlsty, Eunyoung Choi, James R. Goldenring

In gastric carcinogenesis, stomach epithelium undergoes several sequential stages, including atrophic gastritis, metaplasia and dysplasia. Chronic inflammation with alterations in a variety of immune cells and fibroblasts promotes metaplasia progression. However, it remains unclear how diverse fibroblast populations contribute to gastric cancer (GC) development.

Methods: Stomach tissues from 5 GC patients were used for single cell-RNA sequencing (scRNA-seq) to evaluate cellular heterogeneity and classify each type of cell. We performed histopathology and immunofluorescence on gastric tissues for geographical analysis of fibroblasts. Isolated gastroid and fibroblast lines were used for co-culture experiments. **Results:** From scRNA-seq, we obtained 2,709 visible fibroblast transcriptomes that can be divided into four subsets based on the differential gene expression of four genes; *ACTA2*, *PDGFRB*, *PDGFRA* and *FBLN2* (Fig.1A). *ACTA2* was prominently expressed in myofibroblasts which were further divided into two subsets; myofibroblast A and B (MfA and MfB), with MfB also expressing *PDGFRB*. Two fibroblast A and B (FbA and FbB) populations were defined by expression of *PDGFRB* or *FBLN2*, respectively. We examined the distribution of these four different subsets. FbA were located in the isthmus in normal corpus, but expanded throughout to entire metaplastic gland in close proximity with the metaplastic lineages (Fig.1B). In dysplastic or cancerous tissues, FbA cells also surrounded the epithelial compartment, but showed a more disorganized pattern. Expansion of FbB cells appeared at the base of inflamed or metaplastic mucosa associated with lymphoid aggregation. FbB cells were interspersed between metaplastic glands, but were set back from the metaplastic lineages. MfB numbers were dramatically increased only in dysplastic or cancerous tissues, with some association with cancerous lineages. There was no significant change in MfAs in most samples. Based on this observation, we performed co-culture of patient-derived metaplastic gastroids (GOs) with fibroblasts isolated from metaplastic or cancer-derived regions from the same patient. RNA sequencing showed that the metaplasia- and cancer-derived fibroblasts were enriched for FbB and FbA, respectively. Compared to GOs cultured alone, metaplastic GOs cultured with metaplasia-derived fibroblast showed disrupted multilayer growth with higher expression of the dysplasia marker, TROP2 (Fig. 2A and B), indicating metaplasia-derived fibroblasts can promote progression of metaplasia into dysplasia. While cancer-derived fibroblasts increased expression of TROP2 in metaplastic GOs, they also significantly enhanced proliferative activity of metaplastic GOs (Fig. 2C). **Conclusion:** We have identified four gastric fibroblast subsets with distinct geographical distributions and functional heterogeneity in gastric carcinogenesis.

Fig. 1

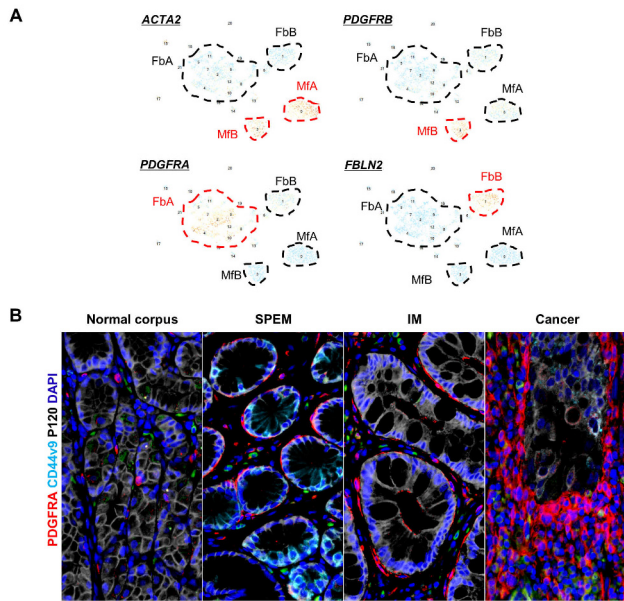


Figure 1. Identification of gastric fibroblast subsets. (A) UMAP plots annotated for distinct fibroblast subsets characterized by differentially expressed genes. (B) Distribution of PDGFRA-positive fibroblasts in different gastric lesions, including normal, spasmolytic polypeptide-expressing metaplasia (SPEM), intestinal metaplasia (IM) and cancer.

Fig. 2

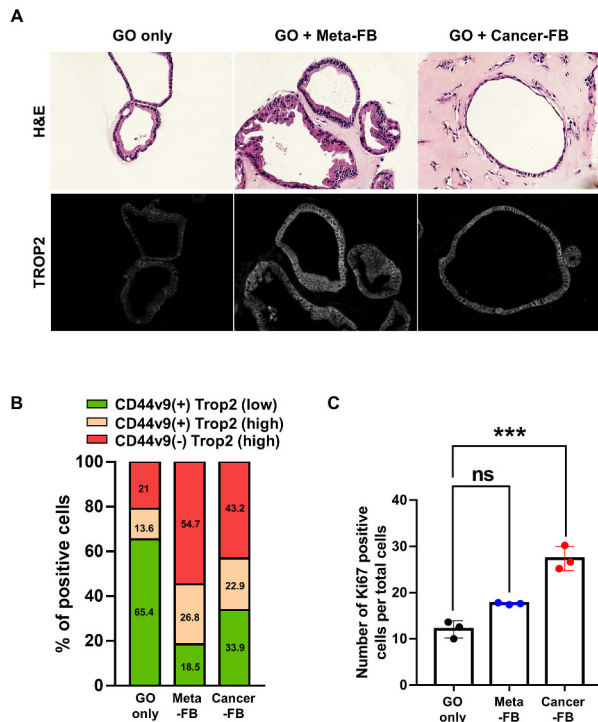


Figure 2. Co-culture of metaplastic gastroids with fibroblasts promotes dysplastic transitions. (A) Hematoxylin and eosin (H&E) staining of GOs and representative images of TROP2 staining. Note that co-culture with metaplasia-derived fibroblasts (Meta-FB) led to both altered morphology in GOs with multilayering of cells, as well as increased expression of TROP2, a marker of dysplastic progression. Cancer-derived fibroblasts (Cancer-FB) did not alter the cystic morphology, but did elicit an increase in TROP2 expression. (B and C) Quantification of CD44v9 and TROP2 expressions (B) and proliferative activity (Ki67) (C) in GOs. Adding metaplastic-derived fibroblasts enhanced TROP2 expression in GOs along with inducing a decrease in CD44v9, a SPEM marker, but did not affect proliferative activity. Co-culture with cancer-derived fibroblast significantly increased proliferative activity with expansion of TROP2-expressing cell proportion in GOs. ***p<0.001.

KRAS ACTIVATION ONLY IN GASTRIC CHIEF CELLS DRIVES METAPLASIA DEVELOPMENT AND PROGRESSION TO DYSPLASIA IN MOUSE STOMACHS

Yoonkyung Won, Brianna M. Caldwell, James R. Goldenring, Eunyung Choi

Introduction Gastric cancer commonly develops within a carcinogenic cascade from pre-cancerous metaplasia to dysplasia and adenocarcinoma. Gastric chief cells are a differentiated cell lineage, that release digestive enzymes and transdifferentiate into SPEM (Spasmolytic Polypeptide Expressing Metaplasia) cells, a major cell population of metaplasia. However, an alternative paradigm has been suggested that gastric isthmal progenitor cells serve as the origin of SPEM cells. We have therefore established a new gastric chief cell-specific driver using GIF gene locus that expresses rtTA from within the endogenous GIF locus (GIF-rtTA) to induce transgenes only in chief cells. We have recently confirmed that the chief cells, rather than isthmal progenitor cells, are the origin of SPEM cells in response to acute mucosal injury. In this study, we generated the GIF-rtTA;TetO-Cre;LSL-K-Ras(G12D) (GCK) mouse allele and examined roles of Kras induction only in chief cells during gastric carcinogenesis. **Methods** The GCK mice at 6 weeks of age were treated with doxycycline water at a concentration of 1 mg/mL of doxycycline (DOX) for 2 weeks to continuously express active Kras in gastric chief cells. Mice were sacrificed at 2, 6, and 10-14 weeks after the DOX treatment. Immunostaining using antibodies against various cell lineage markers was performed to examine changes in the GCK stomachs. **Results** After induction of active Kras expression in gastric chief cells, the GCK mice rapidly developed SPEM positive for AQP5 and CD44v9 within 2 weeks in stomach corpus. These mice progressed to TFF3-expressing IM glands and dysplastic glands positive for CLDN7 as well as Trop2, a novel marker of incomplete intestinal metaplasia (IM) and dysplasia, after 10-14 weeks. Moreover, we examined the expression of CLDN3 was decreased at the base of glands with the dysplastic regions, but a number of MMP7(+) cells, a marker of invasive cells, were increased. These results indicate that active Kras expressed only in chief cells can lead to the full range of gastric carcinogenesis and the GCK mice recapitulate all the phenotypes observed in the Mist1-Kras mice, which induces Kras activation in chief cells as well as in some isthmal progenitor cells. Microenvironment associated with carcinogenesis was established by several types of immune or fibroblast cells during the metaplasia progression. Also, F4/80(+) macrophages and GATA3(+) ILC2 cells were increasingly infiltrated during the metaplasia progression. PDGFRA(+) fibroblasts surrounded metaplastic glands and expanded throughout the metaplasia progression. **Conclusion** Our study indicates that mature gastric chief cells act as an origin of SPEM cells during the gastric carcinogenesis. We therefore conclude that the active Kras expression only in gastric chief cells drives the full spectrum of gastric carcinogenic cascade.

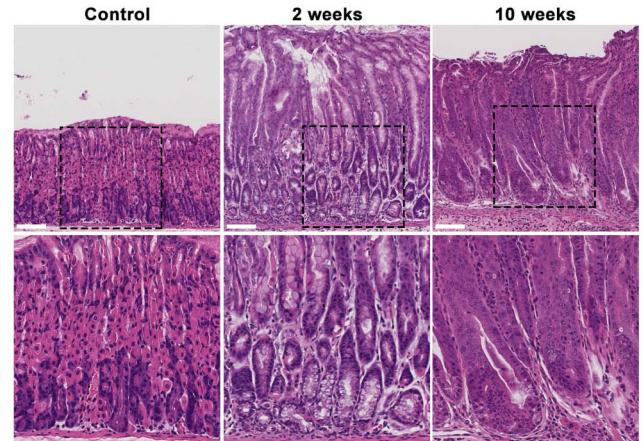


Figure 1. H&E-stained images from GCK mouse stomachs at 2 or 10 weeks after vehicle control or DOX treatment. Dotted boxes denote enlarged regions in the second row. Scale bar: 100 μm

REGULATION OF GASTRIC MUCOSAL HOMEOSTASIS BY R-SPONDIN 3-LGR4 SIGNAL

Ken Kurokawa, Yoku Hayakawa, Mitsuhiro Fujishiro

Objectives: Gastrointestinal stem cells are supported by stem cell niche, and maintain mucosal homeostasis. R-spondin 3 (Rspo3) is one of the key regulators of gastrointestinal stem cells, and is reported to be secreted largely from components of stem cell niche, such as smooth muscle cells, pericytes, or telocytes. Rspo3 binds to leucine-rich repeat-containing G protein-coupled receptors such as Lgr4 and Lgr5, both of which are robustly expressed in gastrointestinal stem cells. In this study, we assessed the effects by Rspo3 signal in gastric epithelial homeostasis by using transgenic mouse models. **Methods:** We used TFF1^{Cre} mice which selectively label gastric epithelial cells, Lgr4^{fllox/fllox} mice, R26^{LSL-rtTA} mice, and newly generated tetO-Rspo3 mice where Rspo3 expression can be induced in a rtTA/doxycycline-dependent manner. Gpr30^{flTA}, KitL^{CreERT}, tetO-Rspo3, and R26^{LSL-rtTA} mice were used for lineage tracing experiments. We performed ISH/IHC to analyze the role of Rspo3-Lgr4 signal in epithelial proliferation, differentiation, and regeneration. Normal and Lgr4-depleted gastric organoids were cultured to validate the effects by Rspo3-Lgr4 signal in vitro. We further performed comprehensive transcriptomic analysis to elucidate molecular changes regulated by the Rspo3-Lgr4 signal in the gastric epithelium. **Results:** Lgr4 was most strongly expressed in the gastric isthmus where gastric stem cells and progenitors reside. Overexpression of